Electrosynthesis of Macroporous Polyaniline−V_2O_5 Nanocomposites and Their Unusual Magnetic Properties

Inna Karatchevtseva, Zhaoming Zhang, John Hanna, and Vittorio Luca*

Institute of Materials and Engineering Science, Australian Nuclear Science and Technology Organisation, PMB 1, Menai, NSW 2234, Australia

Received December 21, 2005. Revised Manuscript Received May 29, 2006

This paper reports a novel two-step one-pot all-electrochemical method for the preparation of interpenetrating conducting-polymer (polyaniline, PANI) semiconducting oxide (V_2O_5) nanocomposites. In the method, a spongy interconnected PANI network is first deposited on a titanium metal substrate. The electrodeposited PANI network has pores on the order of a few micrometers and is used as a template for the V_2O_5 component which is also deposited electrochemically. The dimensionality of the amorphous V_2O_5 that forms can be controlled through control of the current density during the deposition, and this in turn reduces the porosity. As the current density increases and more V_2O_5 is deposited, Raman and X-ray photoelectron spectroscopy (XPS) indicate that the conductivity of the PANI decreases. Regardless of the current density used in the range 1−5 mA/cm^2, the ^{51}V solid-state NMR spectrum of the V_2O_5 component shows a major resonance at about −8500 ppm which is ascribed to a Knight shift due to interaction of the PANI conduction electrons with the ^{51}V nuclear spin. The magnitude of this ^{51}V Knight shift is unprecedented exceeding by a significant margin any of those previously reported for vanadium oxide compounds.

Introduction

The templating of crystalline and/or noncrystalline inorganic oxides to create periodic porous materials has represented a major endeavor in materials chemistry over the past half century. Zeolites (aluminosilicates) are the archetypal microporous material, and many zeolites can be synthesized hydrothermally from aqueous solutions containing an organic structure directing agent and a precursor gel. Silicate and non-silicate mesoporous oxides can likewise be assembled from mixtures of inorganic solution precursors, but in this case the templating agents are larger structures formed by surfactants. The formation of periodic macroporous metal oxide structures requires even larger templates such as large droplet microemulsions,[1] the use of polymer spheres[2−4] recently extended to vanadium phosphates,[5] or the use of polymer membranes.[6] In the present contribution our interest is in the generation of porous conducting polymer transition metal oxide composites at the nano- to macro- length scale and their assembly using electrochemical processes. Application of conducting polymers in electronic devices of the future will require control of the length scale, structure, periodicities, orientation, and morphologies leading to enhanced conductivity and other properties compared with bulk materials.[7,8] Composite materials built from conducting polymers and semiconducting oxides offer exciting possibilities for the generation of novel hybrid properties and applications such as in organic solar cells.

Polyaniline (PANI) is unique among conducting polymers in that it can be rapidly converted between the base (insulator) and the salt form (conductor) by treatment with acid or base or by electrochemical means. PANI also has good environmental stability and can be easily and cheaply produced. It has been intensively studied over the past two decades, and much is known about its structural and electronic properties. Considerable interest has been shown in enhancing the conductivity of PANI by improving order through chemical methods. This can be achieved by using either template[9,10] or template-free approaches. The latter approach can utilize, for example, β-naphthalene sulfonic acid[11] (NSA) or camphor sulfonic acid[12] (CSA) as dopants.

The morphology of electrochemically prepared PANI depends strongly on the experimental conditions including the nature, geometry, and surface preparation of electrodes, the supporting electrolyte, the potential, current density, agitation, sweep rate, and temperature.[13,14] It is clear, therefore, that electrochemical methods of PANI production offer additional variables for control of the polymer morphology and orientation through control of the electric field

* Corresponding author. E-mail: vlu@ansto.gov.au.

(1) Imhof, A.; Pines, D. J. *Nature* **1997**, *389*, 948.
(2) Holland, B. T.; Blanford, C. F.; Stein, A. *Science* **1998**, *281*, 538.
(3) Holland, B. T.; Abrams, L.; Stein, A. *J. Am. Chem. Soc.* **1999**, *121*, 4308.
(4) Holland, B. T.; Blanford, C. F.; Do, T.; Stein, A. *Chem. Mater.* **1999**, *11*, 795.
(5) Carreon, M. A.; Guliants, V. V. *Chem. Mater.* **2002**, *14*, 2670.
(6) Caruso, R. A.; Antonietti, M. *Chem. Mater.* **2001**, *13*, 3272.
(7) Bein, T.; Enzel, P. *Angew. Chem., Int. Ed. Engl.* **1989**, *28*, 1692.
(8) Menon, V. P.; Lei, J.; Martin, C. R. *Chem. Mater.* **1996**, *8*, 2382.
(9) Bartlett, P. N.; Birkin, P. R.; Ghanem, M. A.; Toh, C.-S. *J. Mater. Chem.* **2001**, *11*, 849.
(10) Delvaux, M.; Duchet, J.; Stavaux, P.-Y.; Legras, R.; Demoustier-Champagne, S. *Synth. Met.* **2000**, *113*, 275.
(11) Zhang, Z.; Wan, M. *Synth. Met.* **2003**, *132*, 205.
(12) Long Y.; Chen, Z.; Wang, N.; Ma, Y.; Zhang, Z.; Zhang, L.; Wan, M. *Appl. Phys. Lett.* **2003**, *83*, 1863.
(13) Diaz, A.; Logan, J. *J. Electroanal. Chem.* **1980**, *111*, 111.
(14) Inzelt, G. *J. Electroanal. Chem.* **1990**, *279*, 169.

10.1021/cm052821e CCC: $33.50 Published 2006 by the American Chemical Society
Published on Web 09/08/2006

at the electrode surface in addition to retaining access to the regular solution variables. Thus Liu et al.[15,16] have recently demonstrated how careful control of the electrochemical conditions during deposition can lead to the growth of either unoriented large fibers or aligned nanotubes on substrates such as Pt, Si, Au, and silica.

While PANI is an extremely interesting conducting polymer, vanadium oxide has been extensively studied for its promise as a cathode material in lithium batteries. A number of attempts[17−20] have been made to produce nanocomposites comprising V_2O_5 and PANI basically to increase ion mobility and electronic conductivity of V_2O_5 with the aim of facilitating charge transport in battery electrodes. A large number of inorganic organic nanocomposite materials have been prepared through the redox intercalation of conducting polymer monomer in a redox active lamellar host material. Indeed, the vast majority of PANI−V_2O_5 nanocomposite materials have been prepared by this oxidative polymerization/intercalation of aniline into preformed lamellar V_2O_5 xerogels in which vanadium is generally reduced from V(V) to V(IV).[21] Another solution based method consists of coaddition of a vanadate precursor and aniline monomer.[22] An early study of PANI−V_2O_5 composites has shown that the reduction of V(V) to V(IV) on intercalation needs to be reversed by ozone treatment to achieve good capacity and cyclability of such composite batteries in lithium batteries.[23] Ferreira and colleagues have used this same redox intercalation route to prepare PANI−V_2O_5 battery electrodes that show modest improvements in capacity with respect to theoretical capacity, but it is clear that there is significant room for improvement.[24] To our knowledge no electrochemical routes to the deposition of thick vanadium oxide composites with PANI have ever been published.

Given that the individual components of the composite materials of concern here are either conductors or semiconducting oxides containing redox centers, electrochemically assisted assembly is a viable and interesting option. A number of strategies can be envisaged for the electrochemically assisted assembly of such structures such as first the assembly of the organic matrix or template followed by electrodeposition of the inorganic component or the inverse where the oxide is first formed and then the polymer introduced. It is the former strategy that is of concern in this work.

To our knowledge, very few papers have so far addressed the electrosynthesis of PANI on a Ti surface. The most comprehensive studies of the electrochemical synthesis of PANI on titanium surfaces have been undertaken by Geskin,[25] Abalyaeva and Kogan,[26] and later by Arsov.[27] In these studies, the PANI films consisted of a robust macroporous interconnected open network of polymer fibers. Such a structure can be exploited as a template for the deposition of a semiconducting transition metal oxide such as vanadium oxide. This is expected to produce a composite that would offer the potential advantage of eliminating contacts between PANI containing vanadium oxide particles as occurs with PANI−V_2O_5 composites generated through redox intercalation and polymerization of aniline into preformed particles of V_2O_5 in gel or nanotube form. Electrodeposition of V_2O_5 on the continuous PANI backbone also offers the potential for regulation of the porosity of the macroporous composite through control of the quantity of V_2O_5 deposited.

In this study we explore the possibilities for the simple two-step one-pot electrochemical preparation of the novel PANI−V_2O_5 interpenetrating network by electrochemical means that can in principle afford control of the dimensionality of both conductor and semiconductor.

Experimental Section

Aniline (≫99.5%) and vanadyl sulfate hydrate ($VOSO_4 \cdot nH_2O$, fw = 163) were obtained in high purity from Aldrich Chemical Co., Inc., and used without further purification. Perchloric acid (Ajax Lab Chemicals, 70%) and ethyl alcohol (Aldrich) were also used as received. All aqueous solutions were freshly prepared with Millipore water.

PANI−V_2O_5 nanocomposite films were produced by electrochemical deposition. A conventional three-electrode cell was used in all experiments. Titanium plates of different thicknesses were used as the counter and working electrodes, and Ag/AgCl was used as a reference electrode. Titanium plates were thoroughly washed with ethanol and dried in air before each experiment. All electrochemical measurements were performed using a PGZ 402 model potentiostat by VoltaLab.

The fabrication of PANI−V_2O_5 composite films was carried out in two steps. First, electropolymerization of macroporous PANI films was carried out from 0.25 M aniline solution in 1 M $HClO_4$. PANI films were grown on titanium surface for 1 h under a constant current density of 0.08 mA/cm^2. After deposition, the polymer-coated electrode was washed with 1 M $HClO_4$ to remove small oligomers and the excess monomer and then dried in air at room temperature for 24 h. After this, the PANI film on the titanium substrate was used as a "second-order working electrode" for the deposition of vanadium pentoxide. V_2O_5 was deposited by an

(15) Liang, L.; Liu, J.; Windisch, C. F., Jr.; Exarhos, G. J.; Lin, Y. *Angew. Chem., Int. Ed.* **2002**, *41*, 3665.
(16) Liu, J.; Lin, Y.; Liang, L.; Voigt, J. A.; Huber, D. L.; Tian, Z. R.; Coker, E.; Mckenzie, B.; Mcdermott, M. J. *Chem.—Eur. J.* **2003**, *9*, 604.
(17) Lira-Cantu, M.; Gomes-Romeo, P. *J. Electrochem. Soc.* **1999**, *146*, 2029.
(18) Lira-Cantu, M.; Gomes-Romeo, P. *J. Solid State Chem.* **1999**, *147*, 601.
(19) Li, Z. F.; Ruckenstein, E. *Langmuir* **2002**, *18*, 6956.
(20) Huguenin, F.; Malta, M.; Torresi, R. M. *Electrochem Soc. Proc.* **2001**, *21*, 220.
(21) Kanatzidis, M. G.; Wu, C.-G.; Marcy, H. O.; Kannewurf, C. R. *J. Am. Chem. Soc.* **1989**, *111*, 4139. Petkov, V.; Parvanov, V.; Trikalitis, P.; Malliakas, C.; Vogt, T.; Kanatzidis, M. G. *J. Am. Chem. Soc.* **2005**, *127*, 8805. De, S.; Dey, A.; De, S. K. *Eur. Phys. J. B* **2005**, *46*, 355. Lira-Cantu, M. *J. New Mater. Electrochem. Sytems* **1999**, *2*, 141. Pang, S. P.; Li, G. C.; Zhang, Z. K. *Macromol. Rapid Commun.* **2005**, *26*, 1262. Xu, J.; Li, X.; Liu, J.; Wang, X.; Peng, Q.; Li, Y. *J. Polym. Sci., Part A: Polym. Chem.* **2005**, *43*, 2892. Huguenin, F.; Torresi, R. M.; Buttry, D. A. *J. Electrochem. Soc.* **2002**, *149*, A546. Wu, C.-G.; DeGroot, D. C.; Marcy, H. O.; Schindler, J. L.; Kannewurf, C. R.; Liu, Y.-J.; Hirpo, W.; Kanatzidis, M. G. *Chem. Mater.* **1996**, *8*, 1992.
(22) Ballav, N.; Biswas, M. *J. Appl. Polym. Sci.* **2005**, *96*, 1483.
(23) Leroux, F.; Koene, B. E.; Nazar, L. F. *J. Electrochem. Soc.* **1996**, *143*, L181.
(24) Ferreira, M.; Huguenin, F.; Zucolotto, V.; Pereira da Silva, J. E.; Córdoba de Torresi, S. I.; Temperini, M. L. A.; Torresi, R. M.; Oliveira, O. N. *J. Phys. Chem. B* **2003**, *107*, 8351.
(25) Geskin, V. *J. Chim. Phys.* **1992**, *89*, 1215.
(26) Abalyaeva, V. V.; Kogan, I. L. *Synth. Met.* **1994**, *63*, 109.
(27) Arsov, L. D. *J. Solid State Electrochem.* **1998**, *2*, 266.

oxidative electrodeposition from a 1 M $VOSO_4$ aqueous solution under a constant current density of 1, 2, 3, 4, and 5 mA/cm^2 for 30 min. All experiments were performed at room temperature (22−23 °C).

Scanning electron microscopy (SEM) was used to analyze the topographical features of the nanocomposite films. Samples were coated with carbon prior to examination. The samples were examined with a JEOL 6400 scanning electron microscope. All images were scanned at various magnifications at an accelerating voltage of 15 kV. The microscopic features of the sample were observed with a JEOL 2010F transmission electron microscope operated at 200 kV. Samples were scraped off the substrates, dispersed in acetone, and deposited onto carbon grids.

X-ray photoelectron spectroscopy (XPS) analysis was performed under ultrahigh vacuum with a VG ESCALAB 220i-XL system employing a monochromatic Al Kα (1486.6 eV) X-ray source. The X-ray gun was operated at 120 W, and the spectrometer pass energy was set at 20 eV for regional scans. The diameter of the analysis area was approximately 500 μm, and the thickness of the probed surface layer was around 5 nm. The surface concentrations of different species were determined by integrating the peak area (after subtracting a Shirley-type background) with Scofield sensitivity factors as defined in the software package supplied by VG Scientific. The binding energies were calibrated by fixing the C 1s neutral carbon peak at 284.6 eV. To separate the different N and V components in the N 1s and V $2p_{3/2}$ peaks, each spectrum was fitted with three (N 1s) or two (V $2p_{3/2}$) mixed Gaussian/Lorentzian peaks. The peak position and width, as well as the ratio of the Gaussian and Lorentzian components (G/L), were all allowed to vary freely, but the width and the G/L ratio of the peaks were set to be equal in each fit.

Thermo-oxidative behavior of the PANI−V_2O_5 nanocomposites was examined using a SETARAM TAG 24 in a conventional heating rate mode under air atmospheres at a gas flow rate of 25 cm^3/min. Samples were heated from 25 to 650 °C at a heating rate of 5 °C/min.

The Brunauer−Emmett−Teller (BET) nitrogen adsorption method was used to determine the specific surface area of the films removed form the substrate. Nitrogen adsorption isotherms at 77 K were measured on a Micromeritics ASAP 2010 volumetric adsorption analyzer.

Raman spectra were recorded on a Renishaw Raman imaging microscope (system 3000) with an Olympus metallurgical microscope and a charge-coupled device detector. The samples were excited with the 514 nm line of an Ar laser.

^{51}V solid-state magic-angle spinning (MAS) NMR spectra were acquired using two external magnetic field (B_0) strengths. Spectra of the V_2O_5 gel materials were acquired at 7.05 T (^{51}V spectrometer frequency 78.9 MHz) on a Bruker MSL-300 spectrometer while the spectra of the PANI−V_2O_5 composites were acquired at 9.40 T (^{51}V spectrometer frequency 105.3 MHz) on a Bruker MSL-400 spectrometer. At each field a π/12-acquired pulse sequence was used with a recycle delay of 1 s and a pre-acquisition or dead-time delay of 4 μs. At 7.05 and 9.40 T all experiments were conducted on Bruker 4 mm double-air-bearing probes; at 7.05 T rotational frequencies of 10−12 kHz were implemented while at 9.40 T rotational frequencies of 15 kHz were used. All chemical shifts are referenced to $VOCl_3$ via a secondary reference of 0.16 M sodium metavanadate which was also used for accurate pulse time calibration.

Results and Discussion

Film Morphology and Structure. Typical SEM and transmission electron microscopy (TEM) images of as-prepared PANI films on titanium metal substrates are provided in Figure 1a (and inset). These micrographs show the formation of a macroporous fibrous network structure which consists of interconnecting fibrils with an average diameter around 100−150 nm. A fibrillar structure of this type has been previously observed.[28−30] This interconnected fibrilar structure gives rise to what appears to be a wide size distribution of voids.

The thickness of the films prepared under these conditions is typically a few micrometers (3−5 μm). No surface cracking of the films was observed, and the spongy porous nature of the film was visually evident. The fibril thickness observed by TEM (Figure 1a, inset) was consistent with that observed in the SEM image, and some fibrils appeared broken and disconnected which may be due to the TEM sample preparation method.

These spongy PANI films served as "secondary" electrodes for the deposition of the inorganic component within the structure. It was anticipated that V_2O_5 would be electrochemically deposited on the fibril walls under constant current density conditions.

Indeed, electrodeposition of V_2O_5 on the PANI fibrils resulted in the PANI−V_2O_5 nanocomposite films whose morphology varied according to the experimental conditions, such as current density and deposition time. When low current densities were used (1 mA/cm^2) the fibrillar structure of the PANI−V_2O_5 composite remains similar to that of the parent PANI (Figure 1b). However, when the current density was increased to 3 mA/cm^2, the fibrils appeared to have coarsened, and consequently the void space formed by the fibrilar structure was reduced (Figure 1c). Further increase in current density produced even denser structures with smaller voids as observed by SEM (Figure 1d).

The BET surface area of the films was measured by N_2 porosimetry, and the decrease in surface area of the PAN−V_2O_5 composites was confirmed and is shown in Figure 2. These measurements indicate that the highest surface area was measured for the as-prepared PANI film and is around 5 m^2/g. As the current density increases the thickness of the vanadium oxide film deposited on the fibril walls increases, making these fibrils appear thicker in diameter and shrinking the dimensions of the voids and, hence, the surface area. In fact, the surface area of nanocomposite films decreased from 5 m^2/g for as-prepared PANI to less than 2 m^2/g for the PANI−V_2O_5 film deposited at 5 mA/cm^2 (Figure 2). Although the data is noisy owing to the small mass of sample on these films a clear trend was observed.

The actual vanadium oxide content in the composite system could be easily estimated using thermogravimetric analysis (TGA) results. This calculation was based on the fact that, in flowing air, PANI decomposes completely into volatile products leaving essentially no residue (less than 0.6%) at 650 °C, while the remaining residue reflects the

(28) Wang, B.; Tang, J.; Wang, F. *Synth. Met.* **1987**, *18*, 323.
(29) Kanamura, K.; Kawai, Y.; Yonezawa, S.; Takehara, Z.-I. *J. Phys. Chem.* **1994**, *98*, 2174.
(30) Duic, Lj.; Mandic, Z.; Kovacicek, F. *J. Polym. Sci., Part A: Polym. Chem.* **1994**, *32*, 105.

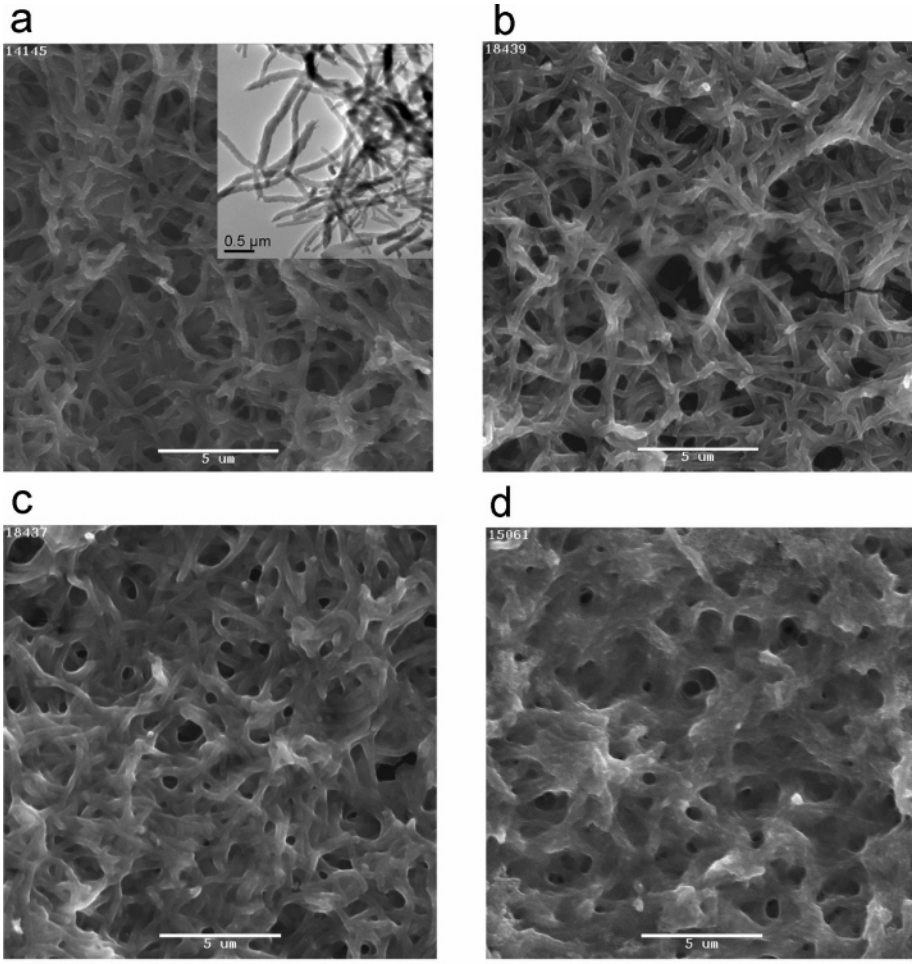

Figure 1. SEM and TEM (a, inset) images of as-prepared PANI film (a) and PANI−V_2O_5 nanocomposites deposited for 30 min as a function of current densities of (mA/cm^2) (b) 1, (c) 3, and (d) 5 (scale bar is 5 μm). The short fibrils observed in part a (inset) are due to sample preparation.

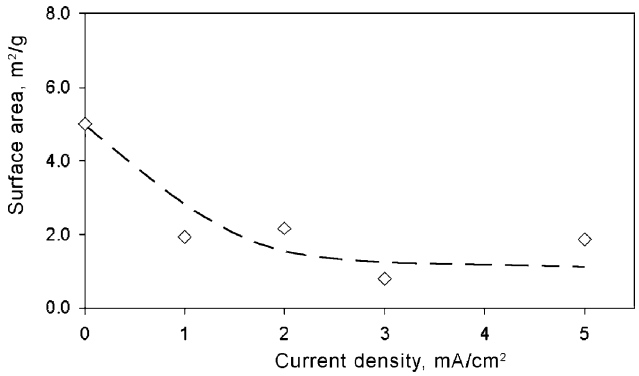

Figure 2. Surface area of the as-prepared PANI film and PANI−V_2O_5 composites as a function of current density.

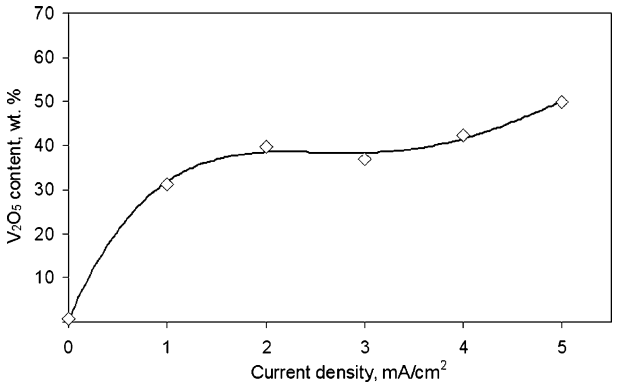

Figure 3. Amount of V_2O_5 deposited on the PANI film as a function of current density (the solid line is a guide only).

vanadium oxide content. It can be seen from Figure 3 that the amount of vanadium oxide introduced into PANI increases with increasing current density. Up to 50 wt % of inorganic component could be incorporated into the organic (PANI) matrix at the highest current densities investigated here.

X-ray powder patterns were measured for selected composite films, and these all showed that at no current density was any crystallinity observed. This suggests that the vanadium oxide forms a dense nonparticulate amorphous film on the PANI fibrils, and, therefore, it can be inferred that the observed surface area arises from the voids that are observed in the SEM.

Electronic Properties of PANI−V_2O_5. It is worth remembering at the outset that the generally accepted structure of PANI is $[(-B-NH-B-NH)_y(B-N=Q=N-)_{1-y}]_n$, where B represents a benzoid reduced unit and Q is a quinoid oxidized unit.[31] It is well-known that the *y* value can be varied continuously from 1 to give the completely reduced form, leucoemeraldine, to 0 to give the completely oxidized form, pernigraniline.

The most important form of PANI, which can be doped to the highly conducting state, is emeraldine, which consists

(31) Salaneck, W. R.; Lundstron, I.; Huang, W. S.; MacDiarmid, A. G. *Synth. Met.* **1986**, *13*, 291.

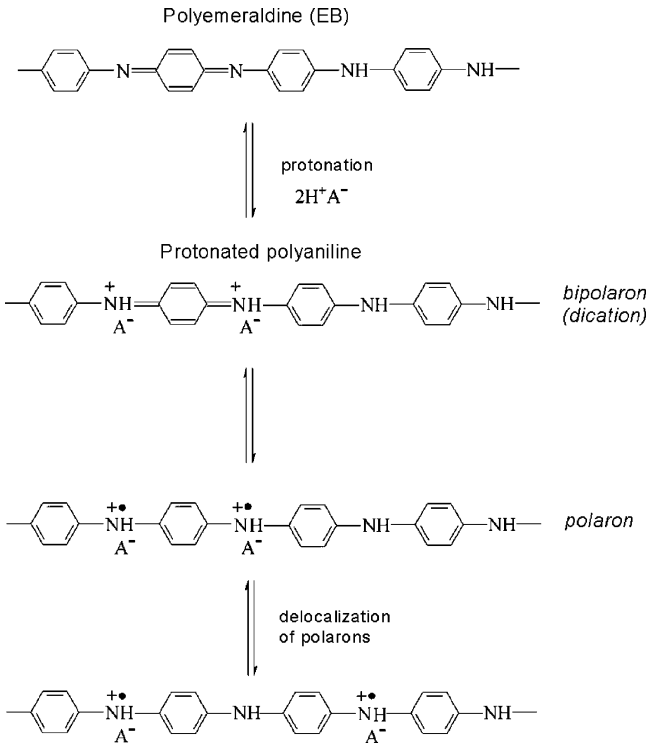

Figure 4. Doping of emeraldine with protons to form the conducting emeraldine salt (protonated PANI).

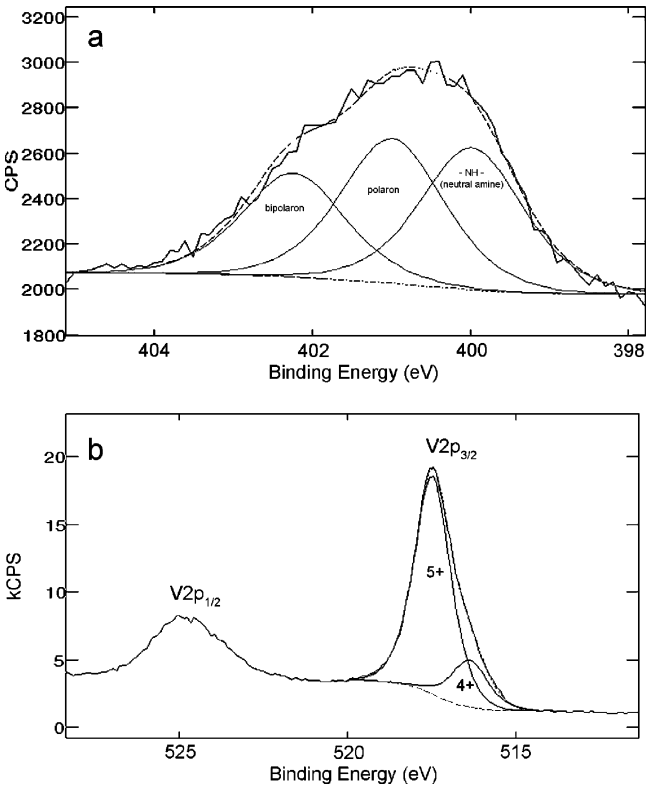

Figure 5. N 1s XPS spectrum for as-prepared PANI film (a) and V 2p XPS spectrum for a PANI−V_2O_5 nanocomposite films deposited at 5 mA/cm^2 for 30 min (b).

of amine (—NH—) and imine (═N—) sites in equal proportions ($y = 0.5$). The conversion to a conductive form can be accomplished by either protonic or electronic doping. For example, the imine sites can be protonated by acids to form the bipolaron (dication salt) with further rearrangements to form the delocalized polaron lattice (polysemiquinone radical-cation salt). The structures formed upon the doping process are shown in Figure 4.

Many factors[32,33] affect the electrical properties of PANI, including the doping and oxidation levels, polaron mobility and concentration, temperature and humidity, film morphology and (importantly) orientation, and the presence of ionic species. The doping level[34] could probably be considered the primary controlling factor of electrical conductivity and other electronic properties of PANI.

The doping level of PANI can be estimated using XPS. The N 1s XPS spectra of PANI can be deconvoluted into three different nitrogen environments with specific N 1s binding energies: <399, 399−400, and >400 eV representing —N═ (quinoid imine), —NH— (benzoid amine), and —N$^{\bullet+}$— (positively charged nitrogen), respectively.[35−38]

The N 1s spectral envelope of the PANI film clearly results from more than a single type of nitrogen (Figure 5a). A minimum of three peaks were required to adequately decompose the spectral envelope using a mixed Gaussian and Lorentzian function. The peak at around 400 eV is attributed to the amine nitrogen of the polymer while the other two peaks at 401.0 and 402.2 eV correspond to positively charged nitrogen. These two different environments at >400 eV can be interpreted, in order of increasing binding energy, as polaron and bipolaron states, respectively.[39] The absence of neutral imine (—N═) species is totally unambiguous because there is no intensity around 398.2 eV. These results, therefore, suggest a high level of doping in the as-prepared PANI film containing no vanadia. In other words the polymer is initially in the emeraldine salt (conductive) form.

Doping level is often determined by many researchers as the area ratios of the peaks >400 eV (peaks assigned to the polaron and bipolaron structure) with respect to total nitrogen.[35−39] In this work, calculation of the [N^+]/[N] ratio from the spectral decomposition indicated a doping level of 0.6 for the PANI film. However, it needs to be pointed out here that while we have followed convention in determining doping level, some serious uncertainty exists in the literature over exactly which species are responsible for the electrical conductivity. While some investigators believe that high electrical conductivity of PANI is directly related to the presence of the charged protonated structures, and that includes both polaron and bipolaron structures, created upon the doping process,[40] others argue that polarons are the

(32) MacDiarmid, A. G. *Angew. Chem.* **2001**, *113*, 2649.
(33) Lu, Y.; Li, J.; Wu, W. *Synth. Met.* **1989**, *30*, 89.
(34) Chiang, J. C.; MacDiarmid, A. G. *Synth. Met.* **1986**, *13*, 193.
(35) Kang, E. T.; Neoh, K. G.; Tan, T. C.; Khor, C. S. H.; Tan, K. L. *Macromolecules* **1990**, *23*, 2918.
(36) Kang, E. T.; Neoh, K. G.; Woo, Y. L.; Tan, K. L. *Polymer* **1992**, *33*, 2857.
(37) Kim, B. J.; Oh, S. G.; Han, M. G.; Im, S. S. *Langmuir* **2000**, *16*, 5841.
(38) Carswell, A. D. W.; O'Rear, E. A.; Grady, B. P. *J. Am. Chem. Soc.* **2003**, *125*, 14793.
(39) Han, M. G.; Cho, S. K.; Oh, S. G.; Im, S. S. *Synth. Met.* **2002**, *126*, 53.
(40) Louarn, G.; Lapkowski, M.; Quillard, S.; Pron, A.; Buisson, J. P.; Lefrant, S. *J. Phys. Chem.* **1996**, *100*, 6998.

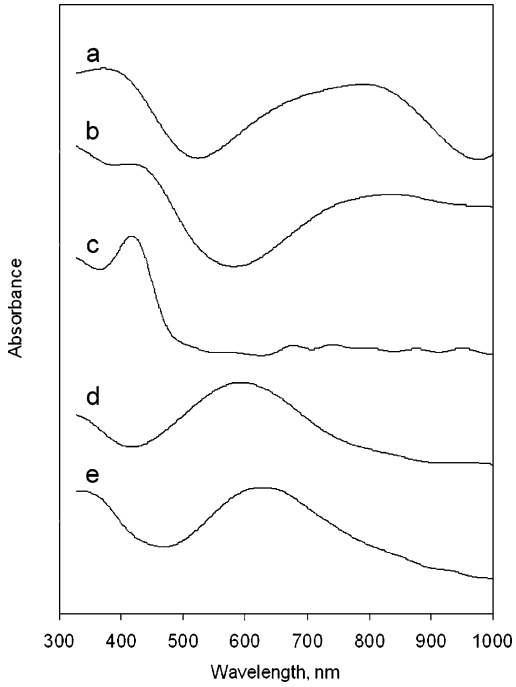

Figure 6. UV−visible spectra of (a) as-prepared PANI and PANI−V_2O_5 nanocomposites deposited for 30 min at different current densities of (mA/cm^2) (b) 1, (c) 2, (d) 3, and (e) 5.

predominant charge carriers responsible for the high conductivity in PANI.[41,42] It has been shown that bipolaron states do exist in PANI, and although theoretical calculations have predicted that the bipolaron state is energetically more favored than the polaron, they are not associated with the conducting regions of the polymer.[43] Therefore, we believe that all the above arguments should be taken into account when estimating the doping level of PANI. If the polaron structures were the only charge carriers, the doping level, in this case, would be 0.4. Our results are in a good agreement with those in the literature which indicate that maximum conductivity occurs when PANI is approximately 50% doped by protons.

To obtain a more complete picture of the electronic state of the series of films, V 2p XPS data were also acquired. Figure 5b shows such a spectrum for a PANI−V_2O_5 nanocomposite film deposited at 5 mA/cm^2. Two peaks, V $2p_{3/2}$ and V $2p_{1/2}$ due to the spin−orbit splitting, were observed at around 517.5 and 524.9 eV, respectively. The results of curve-fitting seem to suggest that the film surface contains predominantly V(V) species and a small amount of V(IV) (shoulder at ∼516.4 eV).[44] This is consistent with the film being comprised of mainly amorphous V_2O_5 with a small amount of unreacted $VOSO_4$.

Apart from inducing interesting variations in morphology and porosity, the deposition of vanadium oxide on the PANI network appears to also influence the electronic state of PANI. The data in Figure 6 show UV−visible spectra recorded for PANI and its nanocomposites with V_2O_5 deposited on titanium and then dissolved in chloroform.

It has to be mentioned that PANI has very limited solubility in most organic solvents. The best organic solvent found for PANI is *N*-methyl pyrrolidine (NMP). However, a large excess of NMP leads to the de-protonation of the emeraldine salts to emeraldine base. This is due to the C═O groups in NMP that form hydrogen bonds with the dopant acid and inhibit the doping process.[45] In fact, the color of the solution turned from green to blue, indicating the de-protonation of the emeraldine salt. Thus, NMP was avoided and chloroform was used instead.

The UV−visible absorption spectrum of as-prepared PANI represented in Figure 6a shows two major absorption bands: a localized polaron band at around 800 nm and a second polaron absorption band at around 400 nm.[46−48] These peaks are characteristic of emeraldine salt and, therefore, as-prepared PANI is in its most conductive state.

The data in Figure 6 also show UV−visible spectra for PANI−V_2O_5 nanocomposites prepared under various deposition conditions. The film on which vanadium oxide has been deposited at 1 mA/cm^2 (Figure 6b) also shows two major UV−vis peaks: localized broad polaron band at around 800 nm and shoulder-like second polaron absorption at 400 nm.

In contrast, only the secondary polaron band at 400 nm could be clearly seen in the absorption spectrum of PANI−V_2O_5 deposited at 2 mA/cm^2 as shown in Figure 6c. The broad absorption between 700 and 800 nm could indicate the disruption of the charge carriers over the polymer backbone.

Further increase in current density led to a significant shift in absorption bands. In the UV−visible spectra of PANI−V_2O_5 deposited at current density 3 mA/cm^2 and higher (Figure 6d,e) the peaks characteristic of PANI appeared at around 600 nm representing the intramolecular transition between the quinoid and benzoid segments in PANI and a shoulder-like band at 360−380 nm which is due to the $\pi-\pi^*$ transition along the polymer backbone.[49] It has to be pointed that there is some ambiguity in the assignment of these bands, particularly the band at 600 nm; however, most researchers accept that this band depends on the oxidation state of polymer and is consistent with the emeraldine base form of PANI, which is an insulator. Additionally, the vanadium (V) oxide charge-transfer band can also appear at around 380 nm.[50] That no V(V)−V(IV) intervalence band is observed in the UV−vis is also evidence that the bulk of the vanadium in the oxide is in the form of vanadium(V).

Thus, in summary, the UV−vis data suggest that increasing current density results in increased doping level and a conversion from a conducting to a less conducting state.

(41) Wallace, G. G.; Spinks, G. M.; Kane-Maguire, L. A. P.; Teasdale, P. R. *Conductive electroactive polymers: intelligent materials systems*, 2nd ed.; CRC Press: Boca Raton, 2003.
(42) Nakajima, T.; Kawagoe, T. *Synth. Met.* **1989**, *28*, C629.
(43) Bonnel, D. A.; Angelopoulos, M. *Synth. Met.* **1989**, *33*, 301.
(44) Colton, R. J.; Guzman, A. M.; Rabalais, J. W. *J. Appl. Phys.* **1978**, *49*, 409.
(45) Pruneanu, S.; Veress, E.; Marian, I.; Oniciu, L. *J. Mater. Sci.* **1999**, *34*, 2733.
(46) Cao, Y.; Smith, P.; Heeger, A. J. *Synth. Met.* **1989**, *32*, 263.
(47) Ito, S.; Murata, K.; Teshima, S.; Aizawa, R.; Asako, Y.; Takahashi, K.; Hoffman, B. M. *Synth. Met.* **1998**, *96*, 161.
(48) Huang, J.; Wan, M. *J. Polym. Sci., Part A: Polym. Chem.* **1999**, *37*, 1277.
(49) Lee, J. Y.; Su, X. H.; Cui, C. Q. *J. Electroanal. Chem.* **1994**, *367*, 71.
(50) Guerra, E. M.; Brunello, C. A.; Graeff, C. F. O.; Oliveira, H. P. *J. Solid State Chem.* **2002**, *168*, 134.

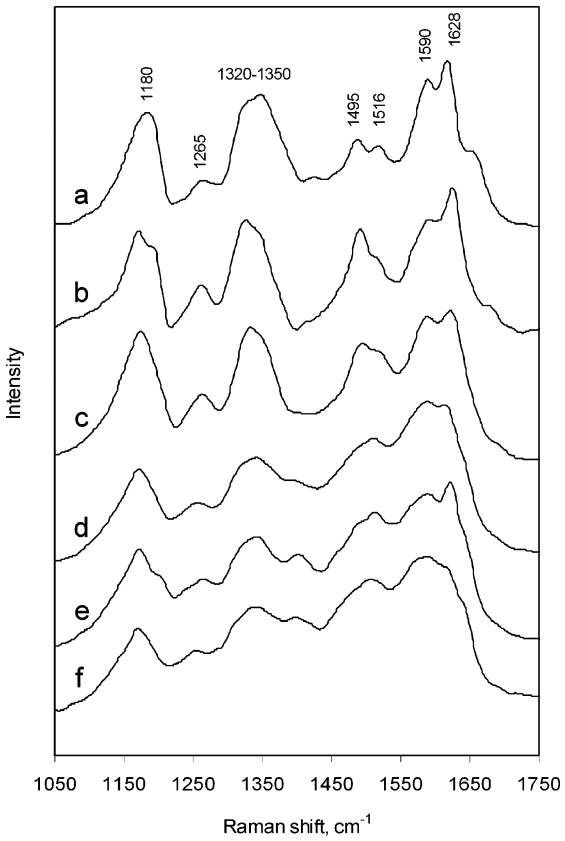

Figure 7. Raman spectra of the as-prepared PANI film (a) and PANI−V_2O_5 composites deposited for 30 min at different current densities of (mA/cm^2) (b) 1, (c) 2, (d) 3, (e) 4, and (f) 5.

Table 1. Raman Peak Positions in PANI and PANI−V_2O_5 Composites[40,52,57−59]

wavenumber, cm^{-1}	assignment
1180	$\delta_{(C-H)}$ in-plane in B ring
1265	$\nu_{(C-N)}$ in the Q ring (semiquinoid and quinoid structures)
1320−1350	$\nu_{(C-N^{\bullet+})}$ in the B ring (polaron structure)
1495	$\nu_{(C=N)}$ in the Q ring (semiquinoid and quinoid structures)
1516	$\nu_{(C-N)}$ in the B ring
1590	$\nu_{(C=C)}$ in the Q ring
1628	$\nu_{(C-C)}$ in the B ring

Raman spectroscopy has also become a valuable tool for characterizing the electronic and structural properties of PANI upon the introduction of V_2O_5. Raman spectroscopy allows the distinction of the different states of PANI involving both oxidation and protonation. The 1100−1800 cm^{-1} region was of particular interest as predominate PANI bands are located in this region. Raman spectra for as-prepared PANI and its nanocomposites with V_2O_5 are shown in Figure 7.

The strongest Raman bands appear at 1180, 1265, 1320−1350, 1495, 1516, 1590−1595, and 1628 cm^{-1} for all samples under investigation. Peak assignments are given in Table 1.

For the as-prepared PANI film the main Raman bands are at 1180, 1330, and 1628 cm^{-1}. Peaks at 1320−1340 as well as a peak at 1516 cm^{-1} are inherently associated with the formation of the semiquinoid radical cation (polaron) during the doping process. Strong bands at 1180 and 1628 cm^{-1} are ascribed to C−H in-plane bending and C−C stretching in the B ring, respectively.

It has to be pointed that other peaks at 1495 and 1590 cm^{-1} were also observed. These peaks are usually assigned to the stretching vibrations of C═N and C═C in quinoid rings, respectively. However, as XPS previously showed, there was no neutral imine (−N═) in as-prepared PANI film surface, and, therefore, it is possible that these peaks are originated from the bipolaron structures. Additionally, the 1265 cm^{-1} band is also often interpreted as characteristic of emeraldine salt (doped PANI) and related to the bipolaron structure.[51] It is clear, therefore, that the electrochemically deposited PANI film is in its conducting state due to high intensity of the 1330 cm^{-1} band related to the C−N$^{\bullet+}$ (polaron) stretching.

Figure 7b−f also shows the Raman spectra of the PANI−V_2O_5 nanocomposite films with V_2O_5 deposited at different current densities. With the current density increasing from 1 to 5 mA/cm^2 important changes occurred in the Raman spectra. It can be seen from Figure 7 that the relative intensity of Raman bands characteristic of a semiquinoid radical cation (bands at 1330 and 1628 cm^{-1}) decreased and, in contrast, the bands characteristic of a quinoid (1495 and 1590 cm^{-1}) ring increased. These changes are more pronounced in the spectra of PANI−V_2O_5 films deposited at the current density of 3 mA/cm^2 or higher (Figure 7d−f). This clearly indicates the transition (oxidation) from semiquinoid to quinoid rings, and, therefore, semiquinoid radical cations are considered to be de-protonated.

Increase in the oxidized (Q) units usually results in the decrease of electrical conductivity of PANI. Therefore, the PANI−V_2O_5 films deposited at current density of 3 mA/cm^2 and higher are likely to be less conducting as the peaks associated with quinoid structures become dominant in Raman spectra of these nanocomposites (Figure 7d− ═f). These results are in a good agreement with previously described UV−vis data.

Another noticeable difference in Raman spectra between PANI−V_2O_5 composites and as-prepared PANI film is the changes in the peak profiles. It can be seen (Figure 7) that the introduction of V_2O_5 into the PANI structure changes the general profile of spectra in the 1000−1800 cm^{-1} region compared with the as-prepared PANI. The peaks become broader with the increasing V_2O_5 content. The broad bands (peaks at 1330, 1490, and 1595 cm^{-1}) indicate that the structure of the C−N$^{\bullet+}$ units in the PANI−V_2O_5 composites is not uniform, but various units of electron-delocalized structures are formed.[52] Comparison of the spectral pattern around 1330−1490 cm^{-1} clearly indicates that the structures of the CNC linkage in the C−N$^{\bullet+}$ unit are more homogeneous, and the electrons are more delocalized in the as-prepared PANI film compared with the PANI−V_2O_5 composite films.

Additionally, Raman bands characteristic of V_2O_5 species were also observed (not shown here). The vanadium stretch ($\nu_{V=O}$) occurs at around 1000 cm^{-1}.

(51) Han, M. G.; Cho, S. K.; Oh, S. G.; Im, S. S. *Synth. Met.* **2002**, *126*, 53.
(52) Ueda, F.; Mukai, K.; Harada, I.; Nakajima, T.; Kawagoe, T. *Macromolecules* **1990**, *23*, 4925.

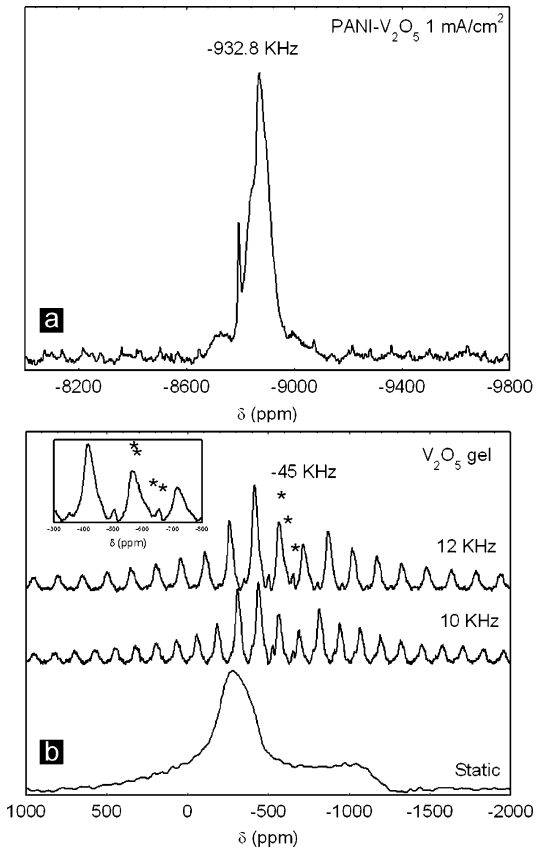

Figure 8. ^{51}V NMR spectra of (a) PANI−V_2O_5 composite deposited at 1 mA/cm^2 and (b) V_2O_5 gel.

So while there is, within experimental uncertainty, little change in the PANI electronic state observed at lower current density deposition of V_2O_5, it seems that on increasing the current density the V_2O_5 content increases (see TGA results earlier) and that this in turn brings about a transition from the conducting to the less conducting state as a function of the doping level.

Samples of the PAN−V_2O_5 composite were examined by ^{51}V MAS NMR spectroscopy at a field of 9.4 T, and the spectrum for a PANI−V_2O_5 composite deposited at 1 mA/cm^2 is presented in Figure 8a. For comparison, spectra of a V_2O_5 gel dried at 50 °C and recorded at 7.1 T and various spinning speeds are also included (Figure 8b). The brown lamellar V_2O_5 gel material was produced by ion exchange of ammonium vanadate solution. The spectrum of the V_2O_5 gel consists of a number of species labeled V1−V4 (−654, −610, −570, and −563 ppm). This spectrum is similar to that reported recently for V_2O_5 gels produced from peroxovanadate solutions. In such gels, isotropic shifts are observed at −623 ppm (V1), −664 ppm (V3), −593 ppm (V2 and V4), and −572 ppm (V5)[53,54] and have subsequently been assigned to unhydrated and hydrated vanadate species in the polymeric V_2O_5 layer structure.[55] On the other hand, as noted in ref 55, other researchers have observed quite different ^{51}V MAS NMR spectra from V_2O_5 gels synthesized by different methods.

The major part of the PANI−V_2O_5 spectrum occurs as a group of five resonances centered at about −8867 ppm (−8722, −8792, −8841, −8867, and −8893 ppm) with little or no spinning sideband manifold. A small remnant of a vanadium gel-like spectrum continues to be observed at around 500 ppm. However, this represents a very minor component of the total spectrum. The resonance at −8792 ppm is relatively much sharper than the other resonances in this region, and we assign this to hydrated $H_xVO_3^{2-x}$ species resulting in motional averaging of chemical shift anisotropy. Such species could be acting as counterions for the emeraldine salt form of PANI. It is remarkable that the spectral envelop of the PANI−V_2O_5 which is centered at about −8500 ppm is shifted by more than 8000 ppm relative to the isotropic shift observed in the oxidized form of V_2O_5 gel. Because the PANI in such a composite has been shown to be in the conducting state we assigned the resonances to the nuclear spin of V(V) ($I = 7/2$) interacting with conduction electrons of the previously identified emeraldine salt form of PANI. Therefore, an extremely large Knight shift is observed. We should recall that previous XPS data have indicated that vanadium is mainly present in its highest oxidation state in the electrodeposited vanadium oxide gel and that V(IV) makes only a small contribution. In comparison, a Knight shift of −4788 ppm observed for α-VO_2 is only about half of this value. For this case VO_2 is a mixed valence V(III)−V(V) oxide with monoclinic structure, and its β phase is a semiconductor at room temperature undergoing a transition to the metallic α phase at 67 °C.[56] These results highlight the extremely strong nature of the coupling between the V_2O_5 polymer gel network and the conduction electrons of the conjugated polymer and represent the first such direct evidence for such a strong interaction in a composite of this type. It is important to note that the actual observation of easily measured, reasonably resolved ^{51}V resonances (albeit highly shifted) is further evidence for V(V) being the predominant vanadium oxidation state, as suggested by the XPS results. If significant concentrations vanadium(IV) were still present strong paramagnetic broadening of these resonances would have been expected which may have precluded observation of most of the total vanadium speciation.

Conclusion

Conductive spongy PANI films have been electrodeposited on titanium electrode surfaces, and these structures have then been used as scaffolds on which amorphous vanadium oxide could in turn be electrodeposited. The control of electrochemical parameters allows some control of the thickness of the vanadium oxide component and, hence, the porosity.

(53) Fontenot, C. J.; Wiench, J. W.; Pruski, M.; Schrader, G. L. *J. Phys. Chem. B* **2001**, *105*, 10496.
(54) Fontenot, C. J.; Wiench, J. W.; Pruski, M.; Schrader, G. L. *J. Phys. Chem. B* **2000**, *104*, 11622.
(55) Fontenot, C. J.; Wiench, J. W.; Schrader, G. L.; Pruski, M. *J. Am. Chem. Soc.* **2002**, *124*, 8435.
(56) Nielsen, U. G.; Skibsted, J.; Jakobsen, H. J. *Chem. Phys. Lett.* **2002**, *356*, 73.
(57) Arsov, L. D. *J. Solid State Electrochem.* **1998**, *2*, 266.
(58) Huguenin, F.; Torresi, R. M.; Buttry, D. A.; Pereira de Silva, J. E.; Córdoba de Torresi, S. I. *Electrochim. Acta* **2001**, *46*, 3555.
(59) Efremova, A.; Regist, A.; Arsov, L. J. *Electrochim. Acta* **1994**, *39*, 839.

XPS indicates that the vanadium is predominantly in the fully oxidized state. The conditions under which the vanadium oxide has been deposited on the PANI network to give an interpenetrating network of conducting polymer and semiconductor have a significant influence on the electronic state of the PANI. PANI remains in its most conductive state if the current density used for the deposition of V_2O_5 is lower than 2 mA/cm^2. However, UV−vis and Raman results indicate that if the current density is increased to 3 mA/cm^2 and above the PANI is less conductive.

The interpenetrating network of PANI−V_2O_5 that is formed appears continuous, and the porosity can allow the diffusion of electrolyte (liquid or solid), the incorporation of guest species, and the possibility of unique adsorption properties. It is also clear that the method described here could be generalized to the deposition of other conjugated polymers and oxides provided suitable electrolyte solutions can be prepared. Oxides of interest might include TiO_2, UO_2, MoO_3, CrO_3, WO_3, and the like. Although the PANI network used as a template has no particular order, it should also be possible to use aligned PANI fibers which can be prepared using stepwise electrodeposition processes.[16]

Finally, we show for the first time that in such a composite the coupling of the conduction electrons associated with the PANI network to the unpaired ^{51}V nuclear spin of the vanadium oxide is extremely strong yielding ^{51}V Knight shifts that are twice that of the next largest reported in the literature. We are presently in the process of investigating in detail the influence that electrochemically controlled variations in the conductive state of the PANI have on the ^{51}V spectrum.

Acknowledgment. The authors are indebted to Mark Blackford, Elizabeth Drabarek, and David Cassidy of ANSTO for assistance with the acquisition of the data.

CM052821E